Droop Control of an Islanded Microgrid Using Harris hawks optimization Algorithm

Mohamed A. Ebrahim
Electrical Engineering Department)
Faculty of Engineering at Shoubra, Benha University)
City, Country
mohamed.mohamed@feng.bu.edu.eg

Reham M. Abdel Fattah
Power Electronics and Energy Conversion Department
Electronics Research Institute
Cairo, Egypt
reham@eri.sci.eg

Ebtisam M. Saied
Electrical Engineering Department)
Faculty of Engineering at Shoubra, Benha University)
City, Country
Ebtisam.saied@feng.bu.edu.eg

Samir M. Abdel Maksoud
Electrical Engineering Department)
Faculty of Engineering at Shoubra, Benha University)
City, Country
Samir.abdelmaksoud@feng.bu.edu.eg

Hisham El Khashab
Power Electronics and Energy Conversion Department
Electronics Research Institute
Cairo, Egypt
khashab@eri.sci.eg

***Abstract*—In order to help to solution power-sharing process, keep to frequency and voltage constrained limits in microgrid system. The parameter values must therefore be chosen accurately. Optimization techniques are a hot topic of researchers; hence this paper presents an optimization technique for finding parameter values of system. This paper will apply a version of Harris hawks optimization (HHO) on microgrid to control the power sharing, frequency and voltage. The results of simulation show that the HHO droop controller improves the quality of micro-grid power by ensuring that variability in the control of microgrid frequency and voltage and efficient power sharing occurs that when there is a micro-grid island mode and when there is a load variation.**

Keywords— droop control, microgrid, Harris hawks optimization, power sharing.

I. INTRODUCTION

In the last decade, the electricity demand was increase and in the near future, the demand for electricity will be expected to rise significantly [1]. To meet this projected demand, there is a trend towards renewable energy sources to be used because they are environmentally sound and are considered economically better [1]. This transition in electricity generation from conventional to renewable energy sources (RES) [2]. This has culminated in the development of small-scale power generation systems named microgrids [2]. A microgrid that involves local loads and Distributed generation sources (DGs) [3]. DG systems are ideal for highly reliable electrical power supply [3]. Various types of energy resources are currently available, such as wind turbines (WTs), photovoltaic system (PVS), fuel cell (FC) [4]. It is difficult to connect these renewable resources directly to a utility grid [5]. To solve this problem is used microgrid to make the interface between the utility grid and distributed renewable resources [3]. Microgrid must be worked in the grid-connected mode as well as island mode contingency [3]. The inverter must be used to convert DC to AC. Therefore, an inverter is the main microgrid element [3]. In a microgrid, there are working Inverter parallel. Because if an inverter fails, the remaining modules can still supply the necessary power to the load [3]. The inverters control is intended to deliver the active and reactive energy while preserving the variability in frequency and voltage within the allowable limits [6]. To control inverters used the droop control technique. The droop control technique provides power-sharing, voltage and frequency constrained limits [7]. Such droop controllers are tuned with identical parameters in the d-axis and q-axis by trial-and-error method [8]. Nonetheless, in obtaining optimum parameters or even the right outcomes, this method has a major limitation.

Researchers have a propensity to use optimization algorithms to overcome many engineering problems and challenges. Lately, several types of algorithms have emerged such as of Harris hawks optimization (HHO) [1], Salp Swarm Inspired Algorithm (SSIA) [2], grasshopper optimization algorithm (GOA) [3], Sine Cosine Algorithm (SCA) , Whale Optimization Algorithm (WOA) [4], Moth-Flame Optimization Techniques [5], and Grey Wolf Algorithm (GWO)[6]. X. Bao.Proposed a hybrid technique between HHO and DE [7]. The proposed method could fulfill the real-world and complex task of multilevel thresholding color image segmentation excellently. Touqeer et al. Applied the grasshopper optimization algorithm (GOA) on the islanded microgrid were used to calculate the PI controller gain [3]. Ebrahim et al. Using PSO to measure primary and secondary PI-based droop control coefficients for autonomous microgrid [8]. Although, the Previous literature has been successful in achieving power sharing, However, the researchers did not consider microgrid

droop control uncertainties such as controller gains inaccuracy, system parameter deterioration, and RER uncertainties.

II. Background of HHO

In 2019, Heidari et al proposed a new mathematical model called HHO that inspired them to do so is the nature of the life of the hawks and their behavior in attacking prey [1]. The hawks can be classified as nature's smartest birds. The most important features of the Harris hawk are that it lives in fixed groups and the special cooperative behaviors with other members of the family living in the same cohesive unit. Of the nature of the Harris hawk that is well acquainted with their family members and tries to be aware of their movements during the attack on prey [1]. In this way, the hawks often conduct a " leapfrog " movement throughout the target site. Many hawks try to attack from several directions together and at the same time to besiege prey. The outcome of the previous attack depends on the ability to escape and prey behavior, either the attack can be completed quickly by capturing prey within seconds or the prey will resist, needs here the seven kills may contain multiple, short-length, quick dives nearby the prey during several minutes[1]. The main benefit of this strategy is that the Harris hawks cooperate with each other to reach the prey for their exhaustion, further weakening them. Besides the above, the prey is hard to regain their ability to defend themselves and avoid the hawks attack, often the strongest Harris' hawk catches prey and shares food with the rest of the group [1].

HHO can be applied to any optimization problem because it is a population-based and gradient-free technique. The HHO algorithm also includes including two exploration phases, transition from exploration to exploitation and four exploitative steps [1].

A. Exploration Phase

The exploration phase is that the hawks of the Harris sit randomly in their positions waiting for the prey to be found. The exploration process consists of two strategies [9]. There are two strategies, each with equal chances of choice, through which Harris Hawks improves his position. Which can be explained in detail as follow: a random value of k < 0.5 means that the hawks perch at certain locations depending on the position of other group members, all members can make sure that they are near enough when the intended prey is attacked. On the other side, a random value of k ≥ 0.5 suggests that the hawks perch at tall trees randomly to discover the desert area. [1].

$$Y(t+1) = \begin{cases} \left(Y_{prey}(t) - Y_m(t)\right) - c_3(LB + c_4(UB - LB)) & k < 0.5 \\ Y_{rand}(t) - c_1\left|Y_{rand}(t) - 2c_2 Y(t)\right| & k \geq 0.5 \end{cases} \quad (1)$$

Where Y (t + 1) is the hawks ' position vector in the next iteration, $Y_{prey}(t)$ is the prey's position, $Y_m(t)$ is the average position of the actual population of hawks, $Y_{rand}(t)$ is a hawk's position randomly selected from the current team, c_1, c_2, c_3, c_4, q are random numbers inside (0,1), Y(t) is the hawk's current position vector. UB and LB are the upper and lower bounds of the search space. t is the current counter of iteration [1], [9].

$$Y_m(t) = \frac{1}{N}\sum_{i=1}^{N} Y_i(t) \quad (2)$$

Where $Y_i(t)$ reflects each hawk's position, N shows the total number of members of the team.

B. Transition from Exploration to Exploitation

Since the prey is trying to escape, there is a process between exploitation and discovery called the transition from exploration to exploitation. The prey loses a lot of energy during the prey attempt to escape and puts the prey energy equation as follows [1]:

$$E = 2E_0\left(1 - \frac{t}{T}\right) \quad (3)$$

E_0 changes randomly at each iteration within the interval (−1, 1). When the prey's ability to escape decreases, this means that it is valuable of E_0 decreases from 0 to -1. But when the prey energy increases to escape, this means that the value of E_0 increases from 0 to 1 and T is the max iteration. The exploration phase would be |E| ≥ 1. The step of exploitation would be |E| < 1 [1].

C. Exploitation Phase

In this stage, by attacking the intended prey found in the previous process, the hawks of the Harris manage the surprise pounce. The HHO suggests four possible strategies to design the attack phase. Suppose r is a random number between 0 and 1. Assume r is an opportunity for a prey to escape successfully (r < 0.5) or not to escape successfully (r ≥ 0.5) before sudden jump on prey. Whatever the prey has tried to escape, the prey won't be able to escape most of the time because the hawks will surround the prey in various directions depending on the retained prey energy E. The retained prey energy used to determine the type of besiege if it is soft or hard. In this relation, the soft besiege occurs when |E| ≥ 0.5 and the hard besiege occurs when |E| < 0.5.In fig.1 show the four Exploitation steps[1], [9].

1) Soft besiege

In this case r ≥ 0.5 and |E| ≥ 0.5. Although the prey has enough energy, because of some random hawk jumps, the prey cannot escape the attack. The Harris' hawks encircle the prey quietly to make prey exhausted and then the hawks swoop on the prey. The Harris' hawks action is described as follows [1], [9]:

$$Y(t+1) = \Delta Y(t) - E\left|KY_{prey}(t) - Y(t)\right| \quad (4)$$

$$\Delta Y(t) = Y_{prey}(t) - Y(t) \quad (5)$$

$$K = 2(1 - c_5) \quad (6)$$

where

ΔY(t): is the difference between the position of the prey and the current location of the hawk in iteration t. K is refers to the strength of the prey jump random during the escape. In each iteration, this value changes randomly to simulate the nature of prey movements. $c_5$is a random number of (0,1)

2) Hard besiege

In this case of r ≥ 0.5 and |E| < 0.5. The prey is very exhausted and has low energy to escape. As a result, the hawks are making virtually no effort to catch the prey, and then the hawks are pouncing on the prey. Using the following formula, each hawk upgrades its current location[1], [9]:

$$Y(t+1) = Y_{prey}(t) - E|\Delta Y(t)| \quad (7)$$

3) Soft besiege with progressive rapid dives

In this approach is |E| ≥0.5 but r < 0.5. The prey has enough energy to escape successfully, so before the sudden swoop on the prey, the hawks must create a soft siege. This approach is smarter than the case before. In the HHO algorithm, the theory of levy flight (LF) is used to design a mathematically model that illustrates prey and leapfrog movements. LF is used to represent the zigzag movements of prey during their escape (especially if the prey is considered a rabbit) and the hawks ' irregular, sudden and speedy diving to surround the prey. Hawks try to correct their positions gradually depending on the movements of prey, and therefore the hawks many fast dives around prey. Therefore, to assume that the hawks could evaluate (decide) their next move on the basis of the following rule in Eq 9 [1], [9].

$$H = Y_{prey}(t) - E\left|KY_{prey}(t) - Y(t)\right| \quad (8)$$

In order to determine whether the hawk this movement better or worse, so it compares the possible outcome of such a movement, including the preceding. If the result is unsatisfactory, when they see that the prey is trying to escape and makes a lot of deceitful movements, the hawks begin to make some irregular, sudden and quick dives to approach the prey. The following equation will illustrate this movement [1], [9]:

$$G = H + S \times LF(D) \quad (9)$$

where

D: the dimension of problem

S: a random vector by size 1 × D

LF: the levy flight function

$$LF(x) = 0.01 \times \frac{u \times \sigma}{|v|^{\frac{1}{\beta}}} \quad (10)$$

$$\sigma = \left(\frac{\Gamma(1+\beta) \times \sin\left(\frac{\pi\beta}{2}\right)}{\Gamma\left(\frac{1+\beta}{2}\right) \times \beta \times 2^{\left(\frac{\beta-1}{2}\right)}}\right)^{\frac{1}{\beta}} \quad (11)$$

where

u, v: random values inside (0,1)

β: a default constant set to 1.5

the strategies formulating the hawks ' position vector can be illustrated as follows:

$$Y(t+1) = \begin{cases} H \text{ if } F(H) < F(Y(t)) \\ G \text{ if } F(G) < F(Y(t)) \end{cases} \quad (12)$$

4) Hard besiege with progressive rapid dives

In this way E | <0.5 and r <0.5, The prey has insufficient energy to flee and the hawks are carrying out a hard besiege simultaneously. This approach modernizes hawk sites and resembles that of soft besiege with a gradual rapid dive. The position of team members is updated by reducing the distance between their average position and the prey position. This motion is illustrated by the following equation [1], [9]:

$$Y(t+1) = \begin{cases} H \text{ if } F(H) < F(Y(t)) \\ G \text{ if } F(G) < F(Y(t)) \end{cases} \quad (13)$$

Where H and G are obtained by applying new Eqs rules. (14) and (15) respectively [1], [9].

$$H = Y_{\text{prey}}(t) - E\left|kY_{\text{prey}}(t) - Y_m(t)\right| \quad (14)$$

$$G = H + S \times LF(D) \quad (15)$$

III. Droop control technique of Microgrid

The Turbine Governor (TG) and the Automatic Voltage Regulator (AVR) are used in the conventional power system to keep both the voltage and the frequency within limits. Unfortunately, TG and AVR cannot be used in PVS and FC systems because they are not suitable for these systems. For these reasons, it becomes mandatory to search for another alternative solution. To maintain the voltage and frequency during any change in the load, thanks to the droop control. Microgrid's complete control strategy consists of the following three steps: droop control, power and voltage-current controllers [3]. Fig. 1 Displays the microgrid control strategy, including three steps, which will be explained in detail in the subsections below.

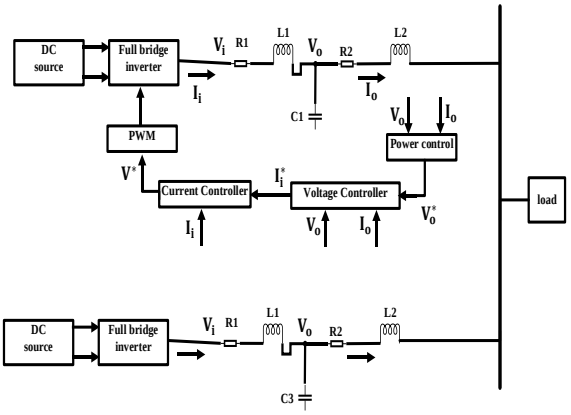

Fig. 1. The system block diagram

a) Power Control

The power circuit consists of the three-phase VSI, the resistive-inductive-capacitive (RLC) filter, the coupling inductor (L_2), and the three-phase load. The RLC filter's most important function is to decrease the high-frequency harmonic to maintain pure sinusoidal voltage. To reduce the coupling between the active and reactive power, the coupling inductor (L_2) is in series with the RLC filter and works as a harmonic damper.

It is important to control Droop that it allows parallel generators to run in a microgrid. Droop control depends on a relationship between active power and frequency, reactive energy and voltage. The droop control has benefits of locally measured data, requires no communication signal, high reliability, simple structure, easy implementation, and various power ratings [3]. In order to calculate the active power (p) and the reactive power (q) before the filter using the output voltage (V_0) and output current (I_0), the V_0 and I_0 are translated into the dq reference frame for calculating (p) and (q) using (16) and (17) [17]:

$$p = V_{0d}\ I_{0d}\ + V_{0q}\ I_{0q} \quad (16)$$

$$q = V_{0d}\ I_{0q}\ + V_{0q}\ I_{0d} \quad (17)$$

For improvement, the p and q will pass in a low pass filter and will be renamed as P and Q. The P and Q are calculated according to (18) and (19), respectively:

$$P = \frac{\omega_c}{S+\omega_c}(v_{0d}\ I_{0d}\ + v_{0q}\ I_{0q}) \quad (18)$$

$$Q = \frac{\omega_c}{S+\omega_c}(v_{0d}\ I_{0q}\ + v_{0q}\ I_{0d}) \quad (19)$$

After calculating P and Q, the reference angular frequency ω and the reference voltage V will be calculated through (20) and (21):

$$\omega = \omega_n - m_p * P \quad (20)$$

$$V = V_n - n_q * Q \quad (21)$$

Where ω_n and V_n are the constant coefficients of frequency and voltage characteristics.

m_p and n_q are the coefficients of static droop.

Thanks to the ability to reduce the voltage drop, there are two parameters that must be controlled: Q and n_q. The Q is uncontrollable because it depends on the load. The n_q must be small. This must therefore be correctly calculated.

b) Voltage-Current Controller

The reference voltage and frequency are used to calculate the reference current (I_i^*) by inserting them into the voltage controller. The current controller will be fed by the output of the voltage controller I_i^*. The current controller output (V^*) feds the pulse width modulation (PWM). The output of PWM is used to control VSI. To calculate I_i^* and V^*, equations (22) and (23) are employed [17].

$$I_i^* = -\omega C_f V_o^* + k_{pv}(V_o^* - V_o) + \frac{K_{iv}}{s}(V_o^* - V_o) \quad (22)$$

$$V^* = -\omega L_f I_i + k_{pc}(I_i^* - I_i) + \frac{k_{ic}}{S}(I_i^* - I_i) \quad (23)$$

Where L_f is the coupling inductor

ω is the cut-off frequency

S is the Laplace transform parameter

Through the PI controller, voltage and current are controlled. The PI controller gains must be correctly calculated. Several approaches are used to calculate PI gains, such as the approach to trial and error and the method of root locus. Such technologies cannot manage complex nonlinear systems such as microgrid or even evaluate the precise gains of controllers. The estimation of PI gains is therefore very important, so this paper will attempt to find the PI controller's optimal gains by applying the HHO algorithm.

IV. Application of HHO in Microgrids

As an optimization tool, the HHO technique has proven successful, so it will be used to evaluate the optimum control parameters and droop control coefficients when load variation occurs. HHO is the technique from which parameter control and parameter control parameters (K_{p1}, K_{i1}, K_{p2}, K_{i2}, K_{p3}, K_{i3}, K_{p4}, K_{i4}, n_q, m_p) can be obtained to eliminate voltage and frequency fluctuations. This process confirms the microgrid's high-power quality and certifies equitable sharing of power. Any technique of optimization requires an objective function to carry out its task. To minimize the error between the measured and required values, this objective function is used. The four types of objective error benchmark functions are expressed by (24)-(27) [10]:

$$\text{IAE}=\int_0^\infty |e(t)|.dt \quad (24)$$

$$\text{ISE}=\int_0^\infty e^2(t).dt \quad (25)$$

$$\text{ITAE} = \int_0^\infty t.|e(t)|.dt \quad (26)$$

$$\text{ITSE}= \int_0^\infty t.e^2(t).dt \quad (27)$$

Where

IAE: integral of absolute error

ISE: integral of square error

ITAE: integral of time absolute error

ITSE: integral of time square error

The ITAE is the most commonly used fitness integration error referred to in the literature because of its easier use and better results compared to its competitors to its contenders like ISE, IAE, and ITSE [10]. Because of the squaring of error, ISE and ITSE are very violent criterions and therefore yield unrealistic performance. However, compared to the ITAE, the IAE is also an inferior alternative because ITAE offers more practical indexing of errors due to the inclusion of the time multiplying error feature.

Fig. 2 Contains a test system diagram consisting of one solar PV array system (SPVA), one fuel cell system (FC), DC-DC boost converter, two battery stations (BSs), supercapacitor (SC), three-phase VSI, load, and transmission line. The microgrid testing system simulates reality by taking into account the effects of transient behaviors on the entire network. The load is shared equally as seen from the MG autonomy given in Fig.2.

one of SPVA and one of fuel cell are used. Moreover, two battery stations each with 56 kW capacity are employed to assist the microgrid power quality. In order to improve the dynamic response of the microgrid, super capacitors will be used because they have the ability to charge and discharge quickly. Using the DC-DC boost transformer incremental conductance (INC) method to monitor the output voltage of the SPVA DC output terminals, the maximum power point tracking point (MPPT) is reached. Table 1 summarizes the parameters of the test system (islanded microgrid model) [11]. MATLAB R2019a codes the HHO for microgrid droop control. Table 2 illustrates a comparison of four types of optimization techniques

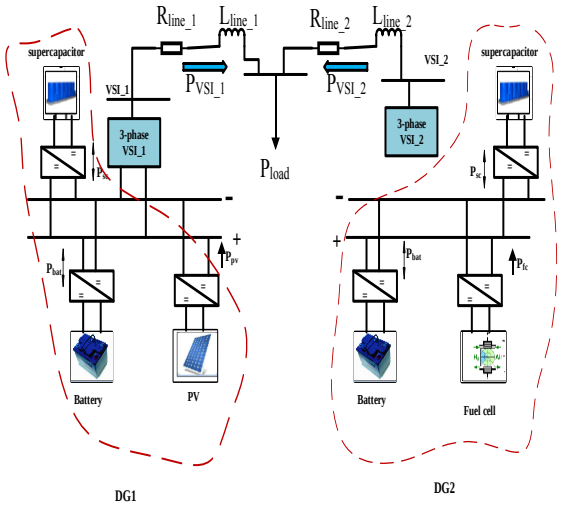

Fig. 2. test system diagram

Table 1 The test system parameters [11].

Parameter	Value	Parameter	Value
V_{base}	380 V	ω_n	1 p.u.

S_{base}	100 kVA	V_n	1 p.u.
ω_{base}	314 red/sec	R_{line1}	0.14 p.u.
L_f	0.95 x10^{-3} p.u.	L_{line1}	2.1 x10^{-3} p.u.
C_f	35 x10^{-6} p.u.	R_{line2}	0.2 p.u.
R_f	0.067 p.u.	L_{line2}	3.5 x10^{-3} p.u.
L_c	0.23 x10^{-3} p.u.	P_{load}	70 x10^3
R_c	0.02 p.u.	ω_c	0.1 p.u.
Ts	5.144 x10-6 sec	Frequency of PWM	10 kHz
Power of PV	109.88 kW	Capacitance of supercapacitor	29 F
Power of battery	56kW	fuel cell	PEMFC - 50 kW - 625 Vdc

Table 2 results of the four optimization techniques

	SSA	PSO	ABC	HHO
Objective function	10.25 x10^6	12.66 x10^6	18.46x10^6	5.86x10^6
K_{p1}	0.6914	0.5579	0.6415	0.4517
K_{i1}	311.4964	475.0824	530.04	257.97
K_{p2}	0.548548	0.513765	0.4707	0.4680
K_{i2}	543.6527	565.1678	349.22	387.77
K_{p3}	11.27808	13.09909	12.225	13.996
K_{i3}	13879.68	12410.52	6358.14	10480.5
K_{p4}	10.25541	13.05646	9.00344	5.41320
K_{i4}	14414.39	11132.63	13267.8	11112.9
n_q	0.272247	0.225909	0.26615	0.31545
m_p	0.014868	0.009724	0.01563	0.01045
Time Taken (min)	207.2686	219.1358	224.480	296.026

V. Case study: Islanding Mode with Changes in Continuous Cyclic Load (IMCCCL)

In this section, RERs variability (variable solar irradiance and temperature) is considered for islanded MG with change of load. Fig.3 Shows solar irradiance from 1000 W / m^2 to 0 W / m^2. Variation of the solar radiation can be interpreted as ramp up / down. Solar radiation is zero at 1.1 to 1.2 seconds, meaning the PV energy is zero so both the battery and the condenser replace the energy. Fig.4 Indicates temperature fluctuations between 25°C and 50°C. The microgrid is operated in insulation mode with continuous cyclic load variations under RER variability as 70 kW (0.7 p.u.) from 0- 0.3 sec, then the load value increased to 110 kW (1.1 p.u.) at 0.3- 0.7 sec, then the load value backs to 70 kW (0.7 p.u.) at 0.7- 1.2 sec, then the load value increased to 110 kW (1.1 p.u.) at 1.2- 1.7 sec, then the load value backs to 70 kW (0.7 p.u.) at 1.7- 2 sec, then the load value increased to 110 kW (1.1 p.u.) at 2- 2.5 sec, finally the load value backs to 70 kW (0.7 p.u.) at 2.5- 3 sec at the end of the load cycle. Fig. 5 Shows that each DG pumps equal amounts of active power into load. Markedly, the rate of power change is approximately the same as the rate of load adjustment, which confirms the strong tracking behavior for droop controllers based on HHO during the scenario of continuous load variations and variations of output power of PV. In addition, voltage and frequency in DGs are preserved within the acceptable limits during the change of output PV and load, as shown in Fig. 6 and 7. Fig. 8 provides insight into how a multi-source energy management scheme is presented by SSIA-PSO based droop control strategy. On top of that, Fig. 8 shows how dynamically SPVAS, BS and SC communicate with each other to preserve supply continuity.

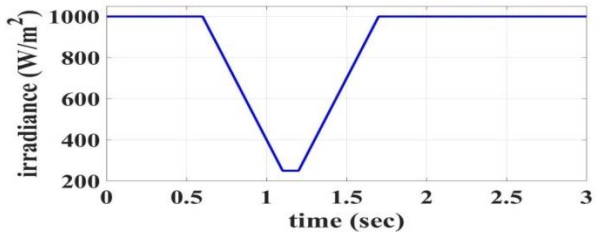

Fig. 3. Solar irradiance variation

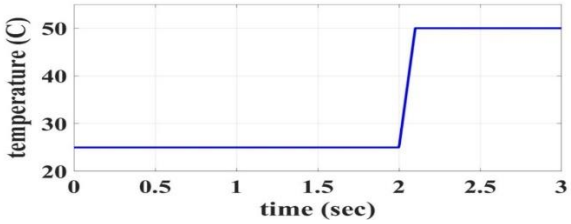

Fig. 4. Solar temperature variation

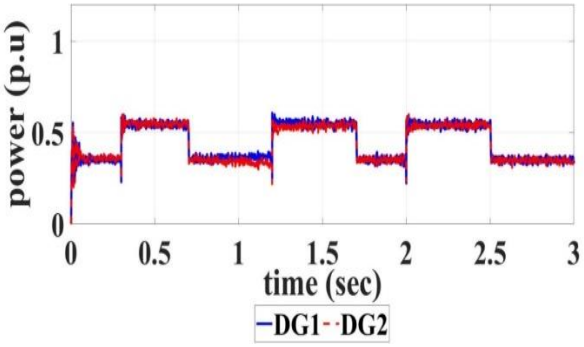

Fig.5 Active powers generated by DGs

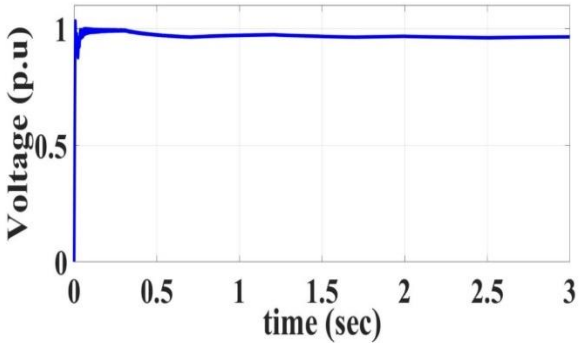

Fig. 6. Voltage magnitude

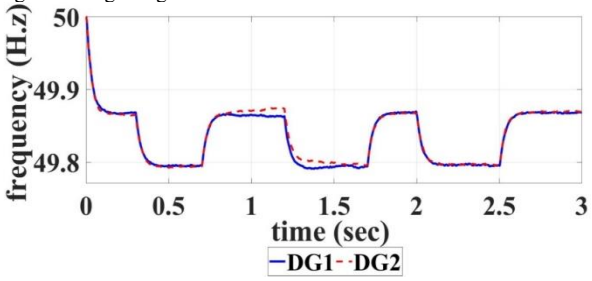

Fig.7 Inverter frequency

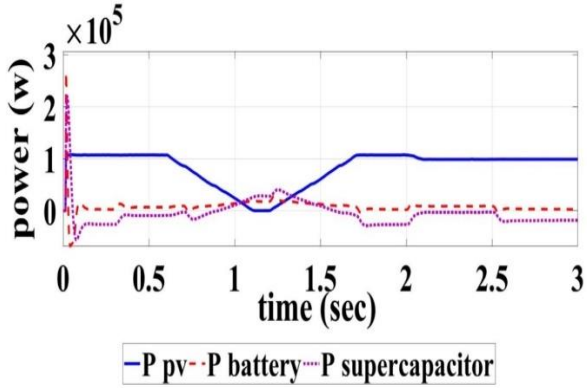

Fig. 8 Powers of SPVASs, BSs, and SC

VI. Conclusion

This paper applied a algorithm for optimisation, HHO. HHO was applied in the field of MG droop control, after proving its efficiency. There are two sources of a microgrid test system. The first source consists of a solar PV array, a battery station (BS), a supercapacitor (SC). The second source consists of a fuel cell (FC), a battery station (BS), a supercapacitor (SC). The HHO is used to calculate PI controller gains and droop control scheme coefficients. The cost function consists of four types: IAE, ISE, ITAE, and ITSE. By applying ITAE as an objective function the best solution is obtained. The comparison with four different types of optimization techniques (SSIA, PSO, ABC, and HHO) applied to the MG scheme confirmed HHO quality as a method of improvement. The obtained gains from PI controllers and the droop control coefficients K_{p1}, K_{i1}, K_{p2}, K_{i2}, K_{p3}, K_{i3}, K_{p4}, K_{i4}, n_q, m_p are implemented in the system. Suggested case include sluggish and rapid shifts in both RERs and load as well as abrupt and ramp variations. Results of the simulation showed that power sharing among the parallel DGs was achieved thanks to the droop control strategy based on HHO. The frequency deviation is within the acceptable range, and with good dynamic response, the DGs are rapidly following load changes. HHO efficacy has been tested by testing many factors that are evaluated during solar radiation, temperature and load changes including the power sharing network, frequency and voltage limits.

References

[1] A. A. Heidari, S. Mirjalili, H. Faris, I. Aljarah, M. Mafarja, and H. Chen, "Harris hawks optimization: Algorithm and applications," *Futur. Gener. Comput. Syst.*, vol. 97, no. March, pp. 849–872, 2019, doi: 10.1016/j.future.2019.02.028.

[2] S. Mirjalili, A. H. Gandomi, S. Z. Mirjalili, S. Saremi, H. Faris, and S. M. Mirjalili, "Salp Swarm Algorithm: A bio-inspired optimizer for engineering design problems," *Adv. Eng. Softw.*, vol. 114, pp. 163–191, 2017, doi: 10.1016/j.advengsoft.2017.07.002.

[3] T. A. Jumani, M. W. Mustafa, M. M. Rasid, N. H. Mirjat, Z. H. Leghari, and M. Salman Saeed, "Optimal voltage and frequency control of an islanded microgrid using grasshopper optimization algorithm," *Energies*, vol. 11, no. 11, 2018, doi: 10.3390/en11113191.

[4] S. Mirjalili and A. Lewis, "The Whale Optimization Algorithm," *Adv. Eng. Softw.*, vol. 95, pp. 51–67, 2016, doi: 10.1016/j.advengsoft.2016.01.008.

[5] S. Mirjalili, "Moth-flame optimization algorithm: A novel nature-inspired heuristic paradigm," *Knowledge-Based Syst.*, vol. 89, no. July, pp. 228–249, 2015, doi: 10.1016/j.knosys.2015.07.006.

[6] S. Mirjalili, S. M. Mirjalili, and A. Lewis, "grey wolf," *Adv. Eng. Softw.*, vol. 69, pp. 46–61, 2014, doi: 10.1016/j.advengsoft.2013.12.007.

[7] X. Bao, H. Jia, and C. Lang, "A Novel Hybrid Harris Hawks Optimization for Color Image Multilevel Thresholding Segmentation," *IEEE Access*, vol. 7, pp. 76529–76546, 2019, doi: 10.1109/ACCESS.2019.2921545.

[8] M. A. Ebrahim, B. A. Aziz, F. A. Osman, and M. N. F. Nashed, "Optimal PI Based Secondary Control for Autonomous Micro-Grid via Particle Swarm Optimization Technique," *2018 20th Int. Middle East Power Syst. Conf. MEPCON 2018 - Proc.*, pp. 1148–1155, 2019, doi: 10.1109/MEPCON.2018.8635217.

[9] B. Description and O. F. The, "A brief description of the drawings !," no. 6, pp. 21–23.

[10] M. H. Marzaki, M. Tajjudin, M. Hezri, F. Rahiman, and R. Adnan, "Performance of FOPI with Error filter Based on Controllers Performance Criterion (ISE , IAE and ITAE)," pp. 5–10, 2015.

[11] M. Kohansal, G. B. Gharehpetian, and M. Abedi, "An optimization to improve voltage response of VSI in islanded Microgrid considering reactive power sharing," *2012 2nd Iran. Conf. Renew. Energy Distrib. Gener. ICREDG 2012*, pp. 127–131, 2012, doi: 10.1109/ICREDG.2012.6190447.